

## Avalanche Behavior in the Dynamics of Chemical Reactions

J. R. Claycomb,<sup>1,2</sup> K. E. Bassler,<sup>1</sup> J. H. Miller, Jr.,<sup>1,2</sup> M. Nersesyan,<sup>3</sup> and D. Luss<sup>3</sup>

<sup>1</sup>Department of Physics, University of Houston, Houston, Texas 77204

<sup>2</sup>Texas Center for Superconductivity, University of Houston, Houston, Texas 77204

<sup>3</sup>Department of Chemical Engineering, University of Houston, Houston, Texas 77204

(Received 4 August 2000; published 5 October 2001)

Sudden bursts of chemical activity, displaying avalanchelike behavior, have been observed in reactions between metals and liquid electrolytes by measuring the time-dependent chemomagnetic fields with a high- $T_c$  SQUID. The observed intermittent chemomagnetic field pulses exhibit power-law behavior in the distributions of peak sizes, noise spectra, and return-time distributions. Such power-law behavior provides evidence for self-organized criticality occurring in the form of “chemical avalanches” over a wide range of size and time scales.

DOI: 10.1103/PhysRevLett.87.178303

PACS numbers: 85.25.Dq, 05.65.+b, 45.70.Ht

The motion of ions and electrons in a chemical reaction generates a magnetic field that can be measured with a high- $T_c$  superconducting quantum interference device (SQUID) [1], providing a sensitive probe of the underlying dynamics. A SQUID magnetometer [2–4] can detect the magnetic fields produced by electrochemical processes in living organisms [5], electrically driven electrochemical reactions [6], and corrosion [7,8]. Here we report on evidence, obtained using a high- $T_c$  SQUID, for avalanchelike dynamics in reactions between metals and liquid electrolytes. We observe intermittent chemomagnetic field pulses, which exhibit power-law behavior in the distributions of peak sizes, noise spectra, and return time distributions. This is characteristic of avalanche behavior in sand [9] and rice [10] piles, superconducting vortices [11,12], microfracturing phenomena [13], and other physical, biological [14–16], and geological [17] systems. The power laws have critical exponents governed by the spatiotemporal evolution of such systems, which are said to exhibit self-organized criticality (SOC) [18]. Complex spatiotemporal behavior has been reported [19,20] for certain reactions, such as the Belousov-Zhabotinsky (BZ) reaction. Hudson [21] gives an extensive review of electrochemical reaction dynamics. A study of noise in electrochemical dissolution reactions is given by Lunt *et al.* [22]. However, there have been no previous reports of SOC in chemical reactions.

We used a high- $T_c$  SQUID to measure the chemomagnetic fields generated by electrochemical currents that flow during the dissolution of metals in liquid electrolytes. The fields were produced by the following replacement reactions of solid magnesium or aluminum with an aqueous cupric chloride solution:



These reactions took place inside a  $2 \times 2 \times 9$  cm Teflon reaction vessel below the high- $T_c$  SQUID magnetometer (Tristan Technologies, Inc., San Diego, CA

92121), which was cooled to 77 K in a G-10 fiberglass liquid nitrogen dewar. Figure 1 shows a schematic of the experimental setup. The entire experiment was shielded from magnetic noise by several layers of high permeability mumetal shielding. During these reaction a 3" long, 3 mm wide, 0.15 mm thick Mg (or 0.5 mm thick Al ribbon) reacted with 25 ml of 1M aqueous  $\text{CuCl}_2$ . Regular domain features were observed in the Mg samples. The metal strip was located at the bottom of the Teflon reaction vessel approximately 2.5 cm from the SQUID pickup loop. The magnetic flux through the  $5 \times 5$  mm<sup>2</sup> SQUID pickup loop, generated by the reactions, was recorded vs time using a digital oscilloscope, and power spectra were obtained from the SQUID

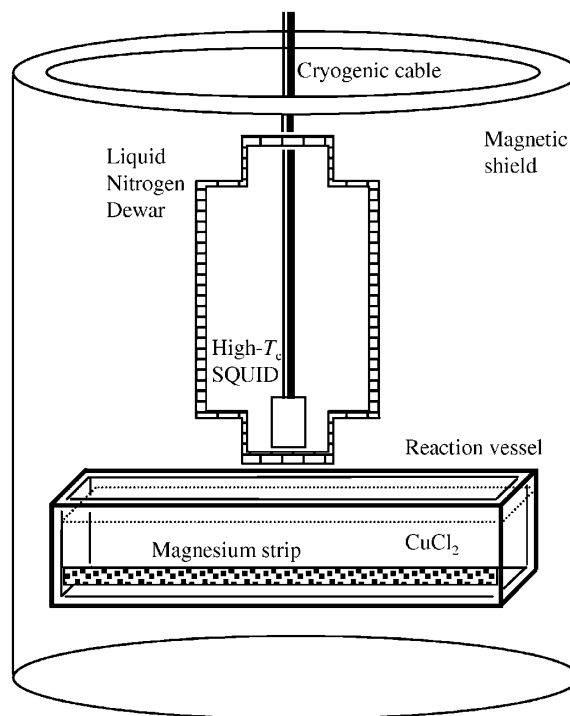


FIG. 1. Experimental setup for chemomagnetic field measurements.

output with a fast-Fourier transform (FFT) spectrum analyzer.

The magnitude of the  $z$  component (vertical component) of the magnetic field  $|B_z(t)|$  produced by reaction (1) is shown for 200 sec in Fig. 2(a). Figure 2(b) shows an expanded view of  $B_z(t)$ , without taking its absolute value, between 100 and 110 sec. The magnetic field peaks are due to sudden bursts of chemical activity or chemical avalanches. Similar time series were recorded during reaction (2). Double-sided histograms show symmetric distributions of positive and negative field peaks due to ionic currents flowing in various directions. The size of each chemical avalanche can be characterized by the magnitude of the corresponding magnetic field peak (up to about 5 nT).

During reaction (1), copper precipitates out of the solution while magnesium dissolves to form aqueous  $\text{MgCl}_2$ . The electrochemical currents that generate the magnetic fields are driven by the ionic reactions  $\text{Mg}(s) \rightarrow \text{Mg}^{2+}(\text{aq}) + 2e^-$  and  $\text{Cu}^{2+}(\text{aq}) + 2e^- \rightarrow \text{Cu}(s)$  at the metal-electrolyte interface. Local reaction and current flow rates are affected by concentration fluctuations [23] in the vicinity of an electrical double layer [24,25] at the interface, by the pitting dissolution of the solid [26], and

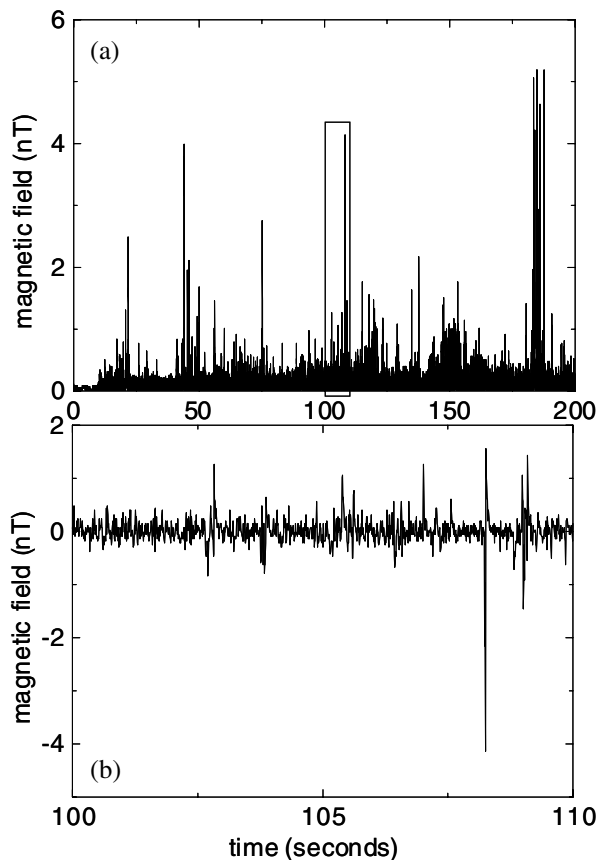


FIG. 2. (a) Magnetic field magnitude recorded with a high- $T_c$  SQUID for 200 sec during the reaction  $\text{Mg} + \text{CuCl}_2 \rightarrow \text{MgCl}_2 + \text{Cu}$ . (b) Expanded view of the “window” between 100 and 110 sec in (a), showing both positive and negative peaks.

by the formation of Cu precipitate layers. Fluctuations in the concentrations of dissolved  $\text{Cu}^{2+}$  and  $\text{Mg}^{2+}$  ions can either locally activate the reaction, which induces transient current flow [26], or inhibit it. The newly formed copper precipitate layers might tend to block the reaction. Pitting dissolution of the surface causes copper layers to break off, thus reactivating the reaction in regions where the Mg surface becomes re-exposed. The system thus appears to contain the ingredients essential [27] for dissipative SOC, namely one or more activation-deactivation processes and dissipation (since energy is dissipated as heat).

Figure 3 shows the magnetic field noise  $S(f)^{1/2}$  recorded during reactions of Mg and Al with 1M  $\text{CuCl}_2$  solutions. Noise data were recorded at least 100 sec after the initiation of each reaction to allow early transient effects to decay while the system attained a “dynamical” equilibrium. The power spectrum  $S(f)$  exhibits  $1/f^\alpha$  behavior where  $\alpha = -\ln S(f)/\ln f \approx 1.8$  for the Mg reaction and  $\alpha \approx 2.0$  for the Al reaction. Such power-law behavior with  $\alpha \approx 2$  occurs in a number of SOC models. We emphasize that uncorrelated (or random) electrochemical processes would give rise to a uniform, “white” noise distribution that is not observed here. Peaks in the noise spectra would be indicative of characteristic time scales, which are not observed in these reactions. Noise spectra were also recorded during reactions of Mg with various concentrations of aqueous  $\text{CuCl}_2$ , ranging from 0.125M to 1.0M. The overall noise level increases with increasing  $\text{CuCl}_2$  concentration.

Figure 4 shows a histogram of the number of magnetic field peaks  $D(B_p)$  as a function of the peak height  $B_p$  for reaction (1). We find that the peaks with sizes  $s = |B_p|$  are distributed according to  $D(s) \propto s^{-\tau}$  for  $s$  between  $2.0 \times 10^{-10} - 5.0 \times 10^{-9}$  T. The slope of the straight line in Fig. 4 gives a critical exponent  $\tau \approx 2.5$ . Deviations from power-law behavior in the low field regime probably

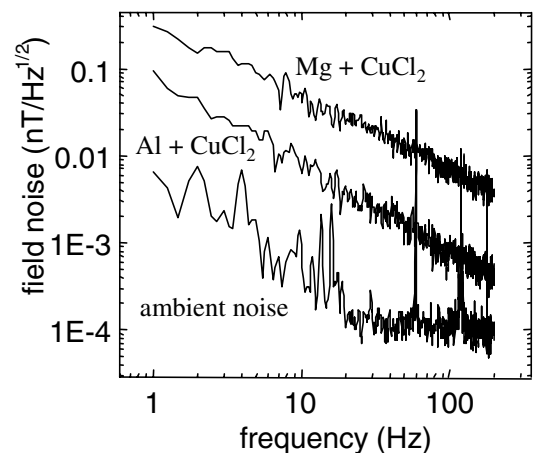


FIG. 3. Magnetic field noise  $S(f)^{1/2}$  recorded during the reactions  $\text{Mg} + \text{CuCl}_2 \rightarrow \text{MgCl}_2 + \text{Cu}$  (top) and  $2\text{Al} + 3\text{CuCl}_2 \rightarrow 2\text{AlCl}_3 + 3\text{Cu}$  (middle). Bottom trace is the ambient noise inside the magnetic shield.

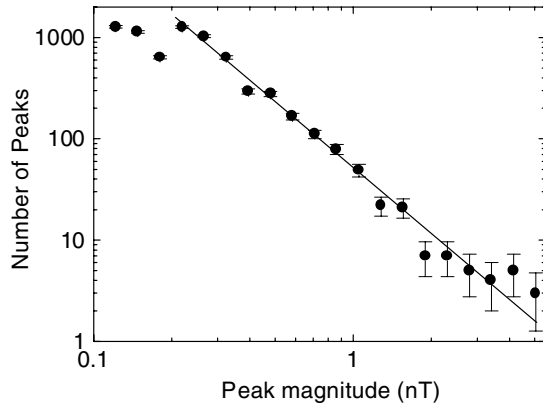


FIG. 4. Distribution of the number of field peaks vs peak magnitude occurring during the reaction  $\text{Mg} + \text{CuCl}_2 \rightarrow \text{MgCl}_2 + \text{Cu}$ . The exponent corresponding to the distribution  $D(B) \propto |B_p|^{-\tau}$  is determined from the slope of the straight line,  $\tau \approx 2.5$ .

result from the environmental noise level  $\approx 100$  pT inside the magnetic shield. The statistics of the high field regime are limited by the total time in which the system evolves, since the largest avalanches occur least frequently. Typical reaction times were on the order of 2000 sec for the tested reactant quantities. Data windows are chosen with 200 sec widths, roughly 1/10 of the total reaction time.

Since the electrolyte concentration and metal quantities steadily decrease as the reaction progresses, the dynamics are not stationary during the entire reaction. However, the system is quasistationary over a sufficiently narrow time window during which only a small fraction of the total reactants are consumed. This was tested by dividing the 200 sec time window used in the experiments in half, and analyzing the data from each half separately. The same power-law exponent  $\tau$  was obtained in each 100 sec subwindow. The influence of sample size on the observed behavior was also studied. No appreciable change in the exponents was observed when repeating the experiment with the Mg coiled into a 0.5 cm pellet.

The distribution of field peaks for the reaction of Al with aqueous  $\text{CuCl}_2$  also exhibits power-law behavior, with a critical exponent  $\tau \approx 3.1$ . The return-time distribution  $D(\Delta t)$  for reaction (1) is shown in Fig. 5. The return time, or forward avalanche size distribution, results from a hierarchical structure of smaller avalanches within larger avalanches [28]. It is defined as the time interval  $\Delta t$  between a magnetic field peak of height  $h$  and the next field peak at least as large, of height  $h' \geq h$ . In Fig. 5 a histogram of the number of return times is plotted vs  $\Delta t$ . The straight line in the log-log plot indicates a power law of the form  $D(\Delta t) \propto \Delta t^{-a}$  for over three decades in time, consistent with SOC. The exponent  $a \approx 0.9$  is obtained from the slope for both reactions of Al and Mg with  $\text{CuCl}_2$ .

A detailed model, based on reaction equations, that predicts SOC behavior remains undeveloped thus far. Here we discuss an interpretation of the Bak-Tang-Wiesenfeld (BTW) model [9] that may capture the essential physics

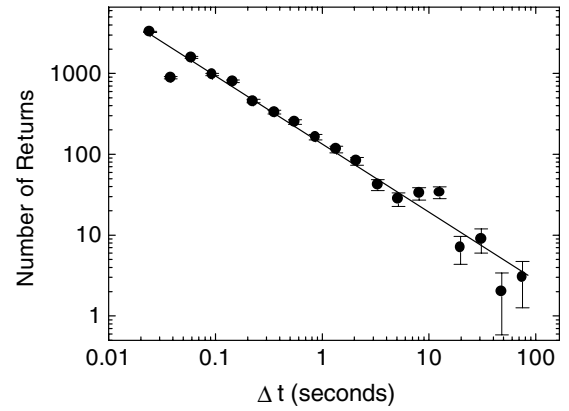


FIG. 5. Return-time distribution  $D(\Delta t) \propto \Delta t^{-a}$  recorded during the reaction  $\text{Mg} + \text{CuCl}_2 \rightarrow \text{MgCl}_2 + \text{Cu}$ . The time intervals  $\Delta t$  are logarithmically binned and the number of returns in each bin is plotted vs  $\Delta t$ . The slope of the straight line yields  $a \approx 0.9$ .

of our experiments during which film growth, breakdown, and repassivation give rise to current fluctuations exhibiting power-law behavior. The BTW model yields a power spectrum exponent equal to 2, in agreement with our measurements. Although the model is highly simplistic, it may serve as a starting point for a more detailed description of SOC related behavior in electrochemical dissolution reactions. In this model, electrochemical reactions take place over a lattice of sites associated with the variable  $z(x, y)$  representing the local passive Cu film thickness. At each time step, a site is chosen at which the Cu film grows according to

$$z(x, y) = z(x, y) + 1. \quad (3)$$

This occurs when a  $\text{Mg}^{2+}$  ion goes into solution after giving up two electrons, which are absorbed by a  $\text{Cu}^{2+}$  ion and deposited as  $\text{Cu}(s)$ . Breakdown events occur when the local film thickness exceeds some critical value  $z_c$ , at which time  $z$  is reset to

$$z(x, y) \rightarrow z(x, y) - 4. \quad (4)$$

The film dendrites then detach from the metal, allowing further ingress of the electrolytic solution. This results in an increased pitting dissolution of the underlying metal and further passive film growth at the 4 nearest neighboring sites, which are updated according to

$$z_{nn}(x, y) \rightarrow z_{nn}(x, y) + 1. \quad (5)$$

Local film regrowth, following a breakdown event, may cause the thickness at neighboring sites to exceed  $z_c$ , triggering additional breakdown/repassivation events. The avalanche continues as Eqs. (4) and (5) are reapplied until the maximum dendrite length is less than  $z_c$ . Film growth continues at new sites according to Eq. (3). Electronic and ionic currents flow during film dendrite growth, with the size of each current fluctuation proportional to the number of sites activated during a given avalanche. Film breakdown events and corresponding current fluctuations may

also be related to the evolution of H<sub>2</sub> bubbles [21] and the charging and discharging of the electrical double layer.

One question deserving attention is the following: In what types of reactions are SOC-like behavior likely to be observed? Also, is avalanche behavior ubiquitous in chemistry or just a rarity? Here we note that sudden bursts of chemical activity, along with  $1/f^\alpha$ -type voltage noise, have long been observed in a class of reactions exhibiting electrochemical noise phenomena. For example, electrochemical noise has been reported in reactions of iron exposed to NaCl solutions [29], aluminum in chloride solutions [30], and during the corrosion of stainless steel in various electrolytes [31]. To date, there is no single theory about the origins and mechanisms of electrochemical noise [31]. Wu *et al.* [32] have proposed a model of cooperative stochastic behavior in localized corrosion, where the probability of pit initiation depends on previous metastable pitting events.

Certain combustion reactions may also exhibit similar behavior. Recently, we have observed  $1/f^\alpha$  noise in the temporal magnetic fields produced by the combustion of several metals in oxygen [33]. These reactions belong to a more general class of self-propagating high temperature synthesis (SHS) reactions [34], where a high-temperature front propagates through a mixture of precursor chemicals converting them into a final product. Rapid magnetic field fluctuations are generated as the combustion front moves through the sample in "bursts." Oscillations in the moving charge distributions probably result from fluctuations in the shapes and instantaneous velocities of otherwise steady reaction fronts. Such reaction front fluctuations have been observed using digital high-speed microscopic video recording [35]. Because of the short duration of these reactions (5–20 sec), and the fact that the combustion wave is moving with respect to the SQUID sensor, a quantitative comparison with the results presented here is not currently possible.

We acknowledge helpful conversations with R. Chu, W. LeGrand, and M. Miller. This work was supported by the Texas Center for Superconductivity, the Texas Higher Education Coordinating Board Advanced Technology Program (ATP), the Robert A. Welch Foundation (E-1221), the UH-ISSO, the NSF through Grant No. DMR-0074613, and the Alfred P. Sloan Foundation.

- 
- [1] M.D. Nersesyan *et al.*, Appl. Phys. Lett. **75**, 1170 (1999).  
 [2] J. Clarke, Nature (London) **372**, 501 (1994).  
 [3] J. Clarke, Sci. Am. **271**, 46 (1994).  
 [4] J. Clarke, Phys. Today **49**, No. 3, 2 (1996).

- [5] J. P. Wikswo, Jr., IEEE Trans. Appl. Supercond. **5**, 74 (1995).  
 [6] B. D. Jette and M. L. A. MacVicar, IEEE Trans. Magn. **27**, 3025 (1991).  
 [7] J. G. Bellingham, M. L. A. MacVicar, and M. Nisefoff, IEEE Trans. Magn. **23**, 477 (1987).  
 [8] A. Abedi, Jr. *et al.*, Rev. Sci. Instrum. **70**, 4640 (1999).  
 [9] P. Bak, C. Tang, and K. Wiesenfeld, Phys. Rev. Lett. **59**, 381 (1987); Phys. Rev. A **38**, 364 (1988).  
 [10] V. Frette *et al.*, Nature (London) **379**, 49 (1996).  
 [11] S. Field *et al.*, Phys. Rev. Lett. **74**, 1206 (1995).  
 [12] K. E. Bassler and M. Paczuski, Phys. Rev. Lett. **81**, 3761 (1998).  
 [13] S. Zapperi, A. Vespignani, and H. E. Stanley, Nature (London) **388**, 658 (1997).  
 [14] P. Bak, K. Chen, and M. Creutz, Nature (London) **342**, 780 (1989).  
 [15] S. C. Manrubia *et al.*, Nature (London) **388**, 764 (1997).  
 [16] P. Bak, Nature (London) **391**, 652 (1998).  
 [17] I. Rodríguez-Iturbe and A. Rinaldo, *Fractal River Basins: Chance and Self-Organization* (Cambridge University Press, Cambridge, 1997).  
 [18] P. Bak, *How Nature Works: The Science of Self-Organized Criticality* (Springer-Verlag, New York, 1996).  
 [19] V. Petrov, Q. Ouyang, and H. L. Swinney, Nature (London) **388**, 655 (1997).  
 [20] A. De Wit, in *Advances in Chemical Physics*, edited by I. Prigogine and S. A. Rice (John Wiley & Sons, Inc., New York, 1999), Vol. 109, pp. 435–513.  
 [21] J. L. Hudson and T. T. Tsotsis, Chem. Eng. Sci. **49**, 1493 (1994).  
 [22] T. T. Lunt *et al.*, J. Electrochem. Soc. **144**, 1620 (1997).  
 [23] R. Kjellander and H. J. Greberg, Electroanal. Chem. **450**, 233 (1998).  
 [24] B. E. Conway, *Theory and Principles of Electrode Processes* (The Ronald Press Co., New York, 1965).  
 [25] G. A. Martynov and R. R. Salem, *Electrical Double Layer at a Metal-Dilute Electrolyte Solution Interface* (Springer-Verlag, New York, 1983).  
 [26] M. Asanuma and R. Aogaki, J. Chem. Phys. **106**, 9930 (1997).  
 [27] P. De Los Rios and Y.-C. Zhang, Phys. Rev. Lett. **82**, 472 (1999).  
 [28] M. Paczuski, S. Maslov, and P. Bak, Phys. Rev. E **53**, 414 (1996).  
 [29] F. Mansfeld and H. Xiao, J. Electrochem. Soc. **140**, 2205 (1993).  
 [30] C. Monticelli *et al.*, J. Electrochem. Soc. **139**, 706 (1992).  
 [31] A. Legat and V. Doleček, J. Electrochem. Soc. **142**, 1851 (1995).  
 [32] B. Wu *et al.*, J. Electrochem. Soc. **144**, 1614 (1997).  
 [33] M. D. Nersesyan *et al.*, Combust. Sci. Tech. (to be published).  
 [34] SHS Bibliography [Int. J. Self-Propag. High-Temp. Synth. **5**, 309 (1996)].  
 [35] A. Varma *et al.*, Proc. Natl. Acad. Sci. U.S.A. **95**, 11 053 (1998).